Microdrilling in Steel with Frequency-doubled Ultrashort Pulsed Laser Radiation

Martin KRAUS, Stephan COLLMER, Steffen SOMMER and Friedrich DAUSINGER

FGSW Forschungsgesellschaft für Strahlwerkzeuge mbH, Pfaffenwaldring 43, 70569 Stuttgart, Germany
E-mail: martin.kraus@fgsw.de

In this paper we study the influence of the processing wavelength on process efficiency and quality at picosecond microdrilling in steel. Possible optical setups for utilizing the second harmonic will be presented, and the influence of wavelength on the drilling rate will be discussed. The potential of helical drilling with the second harmonic in 1 mm thick CrNi-steel will be investigated with regard to process efficiency and hole quality. An analysis will be given of the role of particle-ignited atmospheric plasma and the relation between isophote contour and hole morphology. Our study reveals that a substantial enhancement of both precision and productivity can be achieved by using frequency-doubled instead of infrared radiation. It is shown that plasma ablation and melt production can be minimized by drilling with the second harmonic.

DOI: 10.2961/jlmn.2008.03.0001

Keywords: microdrilling, second harmonic, efficiency and quality, hole morphology, plasma

1. Introduction

The fabrication of high-precision microholes in metals is required in various industrial applications, for example in the field of fuel injection technology. It has been shown in a variety of publications that the use of picosecond laser pulses enables the production of microholes of high quality and contour accuracy without post processing, due to the reduction of melt generation and recast formation to a negligible extent [1-3]. Limiting the pulse energy with the objective of melt reduction and precision enhancement however, leads to insufficient process efficiency [4] resulting in an increase in processing time to several minutes per hole. In order to be competitive in terms of throughput with nanosecond laser drilling and other competing techniques such as wire electrical discharge machining (WEDM), the efficiency of microdrilling with ultrashort laser pulses has to be improved by two orders of magnitude. Thus, the principle object of current research is to raise process efficiency, whilst maintaining highest quality.

The high peak intensity of ultrashort pulses causes a considerable influence of laser-induced plasma on the ablation process. At deep hole drilling, ablated particles accumulate in the gas atmosphere inside the capillary. By interacting with subsequent laser pulses, the residual particles are capable of initiating an electron avalanche which can induce an instantaneous low threshold breakdown of ambient atmosphere even at normal pressure and comparatively low energy densities [5,6]. The so-called particle-ignited plasma builds up inside the capillary and screens a considerable part of the laser radiation. The breakdown threshold at ps drilling amounts to approximately 10^{11} W/cm^2 or a few 10 J/cm^2. It has been revealed by transmission measurements on the basis of through-holes that the time required to lower the particle density by precipitation on the hole walls or removal via convection ranges between several seconds and several minutes. This means that particle-ignited plasma generally plays a role in high aspect ratio microdrilling with ultrashort pulsed beam sources.

Plasma emits a continuous spectrum of electromagnetic radiation caused by bremsstrahlung and recombination. Spectroscopic investigations of the optical emissions during drilling in stainless steel with 5 ps pulses have shown that for deep holes, a continuum can be observed over a period of 100 to 200 ns [7]. Laser-generated plasma can thus be regarded as a secondary source for target heating which is less intense than the laser pulse, but much more long-lasting. This low-intensity post heating can lead to the formation of noticeable melt layers after the termination of the pulse [8,9] and lower quality at ultrashort pulse processing. Moreover, the particle-ignited plasma affects the hole shape as well as the drilling velocity. The magnitude of screening and the period of time that is needed to clear the capillary of particles depends on repetition rate and pulse energy.

It is stated in [10] that for pulse durations above 5 ps, a certain fraction of the pulse energy is absorbed by laser-generated plasma. Absorption by inverse bremsstrahlung is strongly reduced with decreasing laser wavelength ($\alpha \sim \lambda^3$) [11]. Provided that the laser-plasma interaction is governed by inverse bremsstrahlung absorption in the investigated parameter regime, drilling with frequency-doubled laser radiation can be expected to be beneficial from both quality and process efficiency aspects. In addition, frequency-doubled radiation offers better focusability than infrared (IR) radiation. This provides for a larger energy density in the interaction zone and enables a potential increase in productivity [12].

2. Experimental setup

2.1 Laser source

The investigations presented in this work have been carried out using the Staccato laser system manufactured

by Lumera Laser, which is based on the system described in [13]. At the fundamental wavelength of 1064 nm, this diode pumped Nd:YVO_4 oscillator amplifier system generates pulses with a duration of 12 ps at repetition rates between 30 and 100 kHz and an average power of up to 12 W. This average power corresponds to maximum IR pulse energies between 400 and 120 µJ. The Staccato system is equipped with a harmonics generation unit designed to convert the fundamental wavelength into the second harmonic (λ = 532 nm). On doubling the frequency, the pulse duration is compressed to 10 ps. An average power of 5 W is available at 532 nm. During the experiments, the times-diffraction-limit factor M^2 was better than 1.3 at 1064 nm and close to 1.4 at 532 nm. The specified values were read behind the focusing optic, that is to say, at workpiece level. M^2 was measured by means of the camera-based beam propagation analyzer Spiricon M^2-200.

2.2 Processing optics and process technology

In this paper we investigate the influence of the processing wavelength on drilling in sheet metal with a thickness of 1 mm, consisting of X5CrNi18-10 austenitic steel. Fundamental research concerning the average drilling rate and the break-through time has been carried out on the basis of percussion drilling. The main part of the experiments though, has dealt with the fabrication of microholes at a diameter of 100 µm, utilizing a helical drilling process without core.

Helical drilling was performed using the fully automated FGSW Helical Drilling Optic (HDO). Whereas the path diameter and the beam inclination angle were retained constant over all experiments, the rotation frequency of the HDO was adapted to each laser repetition rate. Circular polarization was used to achieve circular hole outlets. All experiments were carried out in ambient air at atmospheric pressure, without extra processing technology.

The inlet and outlet diameters of the microholes were measured by means of an optical microscope. Scanning electron microscope (SEM) images of inlets, outlets and transverse sections of the fabricated holes were recorded to inspect their overall geometry and to obtain information on hole quality.

3. Focusing of fundamental and frequency-doubled radiation

3.1 Basic options for focusing the second harmonic

There are various options for taking advantage of the better focusability of frequency-doubled radiation. The most convenient option is to feed the second harmonic into an unchanged beam delivery system, using the same beam expanding telescope and focusing optic as for the IR radiation. A constant expansion ratio of the beam expander results in a constant diameter D of the incident beam on the focusing optic. Consequently, the focal diameter scales down by a factor of two, according to the bisection of the wavelength. The bisected focal diameter involves a fourfold increase of the energy density, but also a bisection of the Rayleigh length.

If the frequency-doubled beam is expanded to only half the diameter of the incident beam at fundamental wavelength, the very same focal diameter d_f will be produced by a fixed focusing optic. While the focal energy density remains constant, the Rayleigh length doubles, thus producing a slender caustic with a bisected divergence angle. Fig. 1 illustrates the discussed options of focusing the frequency-doubled radiation. The depicted caustics were calculated on the basis of values that approximately correspond to the parameters of the utilized setups. The possibility of operating at extended focal length has not been utilized because changing the focal length modifies the drilling parameters of the HDO.

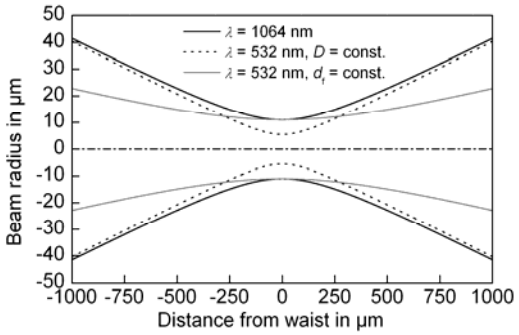

Fig. 1 Calculated beam caustics at fundamental and bisected wavelength for D = const. and d_f = const. λ = 1064 nm or 532 nm, M^2 = 1.3, D = 8 mm or 4 mm, f = 100 mm.

The radius of a Gaussian beam is defined as the radius where the local energy density $H(r,z)$ drops to $1/e^2$ of the maximum value $H_0(z)$ on the beam axis. An increase in axial distance z from the beam waist causes a decline in $H_0(z)$ hence decreasing the local energy density. Consequently, a beam caustic as depicted in Fig. 1 can only be of limited significance in regard to the shape of a laser-drilled hole. A corresponding prediction can rather be derived from the isophotes, that is the constant energy density curves.

The isophote radius in a Gaussian beam can be calculated depending on the chosen isophote energy density H_{Iso}, the axial distance z from the beam waist, the beam waist radius w_0, the pulse energy Q_p and the Rayleigh length z_R. It is given by

$$r(H_{\mathrm{Iso}}, z) = \left(\frac{w_0^2}{2\xi} \cdot \ln\left(\frac{2Q_p \xi}{\pi w_0^2 H_{\mathrm{Iso}}} \right) \right)^{1/2}, \quad (1)$$

where

$$\xi = z_R^2 / \left(z_R^2 + z^2 \right). \quad (2)$$

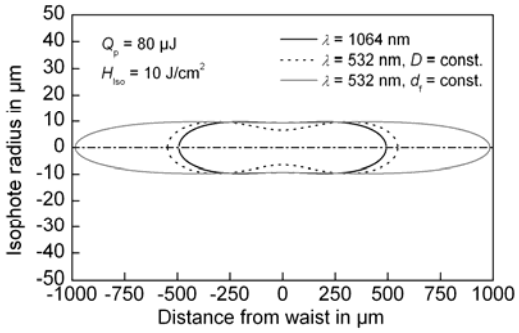

Fig. 2 Calculated 10 J/cm^2 isophotes at fundamental and bisected wavelength for D = const. and d_f = const. λ = 1064 nm or 532 nm, M^2 = 1.3, Q_p = 80 µJ, D = 8 mm or 4 mm, f = 100 mm.

Fig. 2 shows the 10 J/cm^2 isophotes of the beam waists depicted in Fig. 1, calculated with a pulse energy of 80 µJ. The isophote of the fundamental wavelength reaches a length of $z = \pm 500$ µm. For D = const. the isophote of the second harmonic has a similar dimension in z, which is due to the bisected Rayleigh length. In contrast to this, for d_f = const., the 10 J/cm^2 isophote of the second harmonic extends to almost $z = \pm 1$ mm.

It is obvious that normally the energy density acting on the hole wall does not correspond to the isophote energy density. Particularly during the widening phase of the drilling process, the angle between the wavefront normal and the surface normal of the hole wall is close to 90°. As a result the magnitude of the projected energy density, which is determined by the cosine of the angle between the corresponding vectors, can be up to two orders of magnitude lower than the value of the isophote curve. In general however, it can be stated that with the application of frequency-doubled radiation, higher energy densities can either be obtained in the focus (at D = const.) or in the depth of the hole (at d_f = const.). Both options appear desirable with regard to the required improvement of process efficiency.

3.2 Experimental determination of the focal diameter

In order to be able to compare the experimental results obtained at 1064 nm and 532 nm on a firm basis, the focal diameter has not only been calculated, but also determined experimentally for all investigated combinations of wavelength and telescope expansion ratio, according to a method presented in [14]. With this method, the spot diameter of beams with near-Gaussian intensity distributions can be determined by fabricating a series of dimples with energy densities slightly above the threshold value. In producing this series, the ablation diameter d^* is enhanced by gradually raising the pulse energy Q_p. As can be seen from Fig. 3, the focal diameter d_f can be calculated with an accuracy of about 1 µm from the slope of the regression line of $(d^*)^2$ plotted as a function of $\ln(Q_p)$. By measuring the diameter D of the incident beam on the focusing optic, the focal diameters acquired experimentally can be verified using the approximate equation $d_f = (4\lambda \cdot f \cdot M^2)/(\pi \cdot D)$.

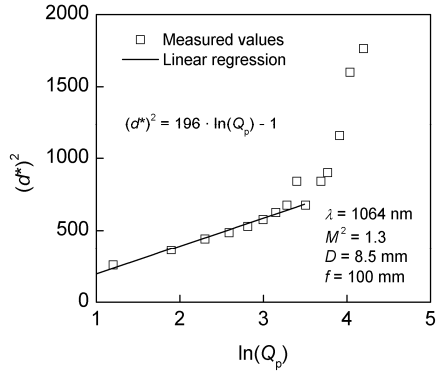

Fig. 3 Experimental determination of the focal diameter at fundamental wavelength according to [14]. The focal diameter can be calculated from the depicted equation of the regression line.

The results of the aforementioned beam diameter measurements are compiled in Tab. 1. At 1064 nm, we generally used a beam expanding telescope with an expansion ratio m of 1:4. Using a beam expander with bisected expansion ratio 1:2 for the second harmonic, the focal diameter was actually kept constant. However, a bisection of d_f was not achieved at constant expansion ratio. This is caused by a reduction of the diameter of the emitted beam and a deterioration of M^2 due to the frequency doubling process.

Tab. 1 Beam diameter on focusing optic D and focal diameter d_f at 1064 nm and 532 nm for D = const. and d_f = const.

λ	1064 nm	532 nm	532 nm
Setup		D = const.	d_f = const.
m	1:4	1:4	1:2
D	8.5 mm	7.6 mm	4.2 mm
f	100 mm	100 mm	100 mm
d_f	19.8 ± 0.6 µm	15.4 ± 1 µm	20 ± 1.1 µm

4. Experimental results

4.1 Drilling rate and completion time

The drilling rate has been investigated by measuring the break-through time at percussion drilling in samples with different thicknesses. The break-through has been detected by means of a photodiode. Subsequently, the acquired drilling times have been assigned to channel depths corresponding to the sample thickness. The drilling rate has not been averaged over the entire channel depth, but calculated in sections according to the gradation of sheet thickness.

As already described in [2], the highest drilling rate is generally obtained at the beginning of the drilling process. A sharp decline of the drilling rate can be observed up to a channel depth of about 500 µm, followed by a phase of constant drilling progression at low drilling rate. From Figs. 4 and 5 it can be seen that the behavior of fundamental (1ω) and frequency-doubled (2ω) radiation differs depending on channel depth and focusing conditions.

For D = const. (see Fig. 4) the capillary tip advances into the workpiece up to 15 times faster at 532 nm than at 1064 nm until a depth of 500 µm is reached. The maximum drilling rate amounts 0.63 µm/pulse at 532 nm and 0.15 µm/pulse at 1064 nm. At channel depths beyond 500 µm, the drilling rate curves converge and eventually

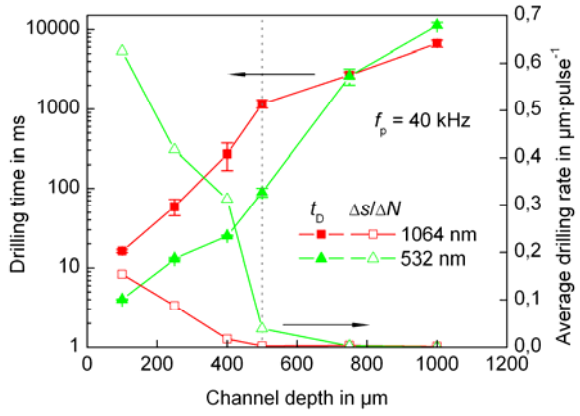

Fig. 4 Drilling time and average drilling rate at 1064 nm and 532 nm versus channel depth for percussion drilling in steel with D = const. 1ω and 2ω: f_p = 40 kHz, Q_p = 80 µJ, f = 100 mm, z_f = -200 µm. 1ω: H = 26 J/cm^2. 2ω: H = 43 J/cm^2. d_f see Tab. 1.

diminish to roundly 1 nm/pulse.

Operating at constant focal diameter, we obtain similar results (see Fig. 5). However, for d_f = const., the maximum drilling rate at 532 nm amounts to only 0.53 µm/pulse. The reason for this is lower focal energy density.

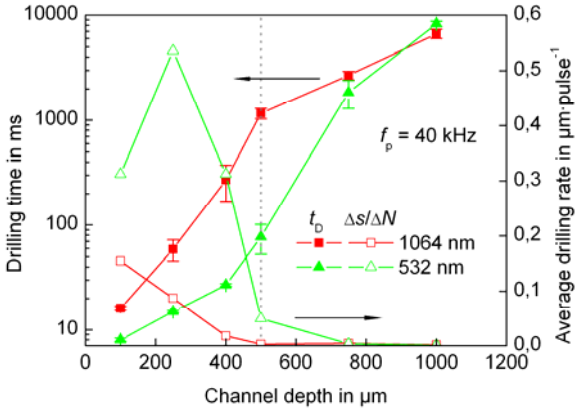

Fig. 5 Drilling time and average drilling rate at 1064 nm and 532 nm versus channel depth for percussion drilling in steel with d_f = const. 1ω and 2ω: f_p = 40 kHz, Q_p = 80 µJ, f = 100 mm, z_f = -200 µm. 1ω: H = 26 J/cm^2. 2ω: H = 25.5 J/cm^2. d_f see Tab. 1.

The completion time, that is the machining time which is needed to complete the desired hole geometry, can be derived from plots of hole diameter versus drilling time. As can be found in Fig. 6, the completion time for a 100 µm hole in 1 mm steel is reduced by a factor of four by means of helical drilling with the second harmonic at D = const. At 532 nm the outlet is widened to 100 µm as early as 60 s after process initiation compared to 240 s at 1064 nm. On top of this, it can be seen that the frequency-doubled radiation widens the outlet to the predetermined diameter at an extraordinarily steady rate. At fundamental wavelength, the outlet diameter tends to fluctuate during the widening phase.

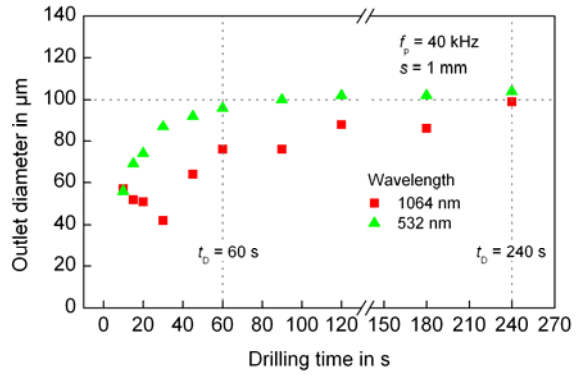

Fig. 6 Outlet diameter versus drilling time for helical drilling in 1 mm steel at 1064 nm and 532 nm with D = const. 1ω and 2ω: f_p = 40 kHz, Q_p = 80 µJ, f = 100 mm, s = 1 mm. 1ω: H = 26 J/cm^2. 2ω: H = 43 J/cm^2. d_f see Tab. 1.

An obvious reason for the increase of productivity by changing to frequency-doubled radiation is the enhancement of energy density in the interaction zone, compare [12]. Another possible explanation is based on the fact that the thickness of the heated material layer is determined by the optical absorption length in machining of metals with ultrashort pulses [8]. As the absorption length is proportional to the wavelength, the pulse energy is deposited in a smaller volume at 532 nm compared to 1064 nm. This, in turn, causes a decline of the threshold fluence and leads to a more efficient widening of the hole by the wings of the Gaussian profile, which is decisive for the formation of the hole shape in the final phase of the drilling process. Measurements presented in [15] confirm the reduction of the threshold fluence with decreasing wavelength. It is shown that the threshold energy density for the ablation of 100Cr6 steel with 10 ps pulses is 63 mJ/cm^2 at 1064 nm and 32 mJ/cm^2 at 532 nm.

According to [11] the calculated absorptivity of pure iron at room temperature and perpendicular incidence is roundly 44 % at 532 nm and 36 % at 1064 nm. However, the absorptivity of laser radiation in metal surfaces does not only depend on wavelength, but also on polarization, workpiece temperature, angle of incidence, alloying elements, surface roughness and oxidation (see [11] for a general discussion). At microdrilling with ultrashort laser pulses, several of the aforementioned influencing values, if at all, are only known within wide limits. Thus it is not clear whether the absorptivity is significantly higher at 532 nm than at 1064 nm in the described experiments.

Recently, high quality holes with a diameter of roundly 90 µm and negative conicity have been manufactured in a 1 mm steel sheet in 30 s [16]. A final estimation whether, in terms of process efficiency, helical drilling should be performed at d_f = const. or D = const. cannot yet be given.

4.2 Quality and hole morphology

Fig. 7 depicts two holes manufactured at 1064 nm and 532 nm, respectively, in a 1 mm CrNi-steel sheet by means of helical drilling. In both cases, the repetition rate was 30 kHz, and the pulse energy was set to 80 µJ, yielding focal energy densities of 26 J/cm^2 at 1064 nm and 43 J/cm^2 at 532 nm. It is obvious that drilling with the second har-

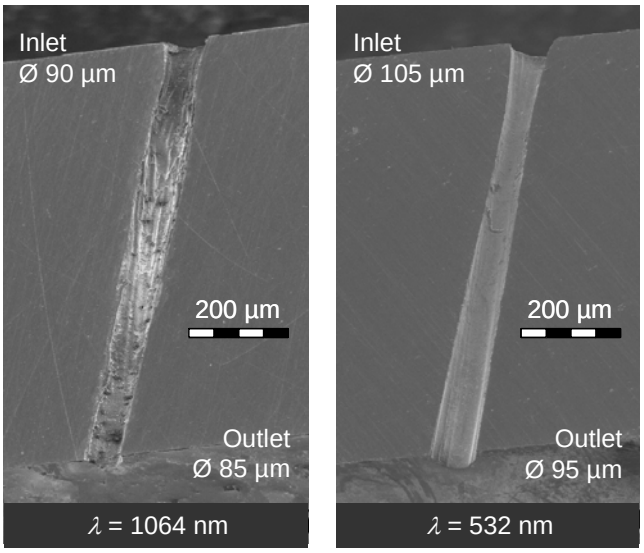

Fig. 7 Transverse sections of microholes in 1 mm CrNi-steel, drilled at 1064 nm (left) and 532 nm (right). 1ω and 2ω: f_p = 30 kHz, f = 100 mm, s = 1 mm. 1ω: t_D = 120 s, d_f = 19.8 µm, H = 26 J/cm^2. 2ω: t_D = 90 s, d_f = 15.4 µm, H = 43 J/cm^2.

monic enables the fabrication of microholes without visible melt deposits and with a regular shape. Contrary to this, at fundamental wavelength, melt ridges are formed on the hole walls, and a burr is generated at the inlet. The formation of melt at 1064 nm explains the bumpy widening behavior as it is displayed in Fig. 6. At 532 nm, with the drilling process not being affected by the irregular melt structures inside the capillary, a smooth development of the outlet diameter takes place.

The depicted holes can also be distinguished by geometrical criteria. Although the machining time was 30 s longer at 1064 nm than at 532 nm, the outlet diameter of the hole fabricated with the IR radiation remains at 85 µm, while the second harmonic widens the outlet to 95 µm, thus producing a negative conical shape. At 1064 nm, the capillary is widened in the upper zone, whereas at 532 nm, the hole shape seems to reproduce the beam waist.

4.3 Congruence of beam shape and hole shape

Fig. 8 shows a comparison of the 5 J/cm^2 isophote contour with the morphology of completed holes in a steel sheet with a thickness of 1 mm. The depicted isophote contours have been calculated on the basis of Eq. (1), taking into account the helical drilling parameters (beam path diameter and inclination angle). Reflection on the hole walls has been neglected because of its minor role in the formation of the capillary during the widening phase. It is apparent that the 1064 nm isophote curve declines to zero shortly above the hole outlet, hence causing the hole walls to curve inwards in the outlet zone. This causes an increase in the normal component of the laser flux, which is achieved by projection onto the hole wall (compare Sec. 3.1), so that ablation proceeds beyond the root of the isophote curve.

The IR radiation ablates the workpiece beyond the isophote, whereas at 532 nm, a good correlation of the isophote contour and hole shape is observed. We believe that the radial expansion at 1064 nm is due to a particle-ignited

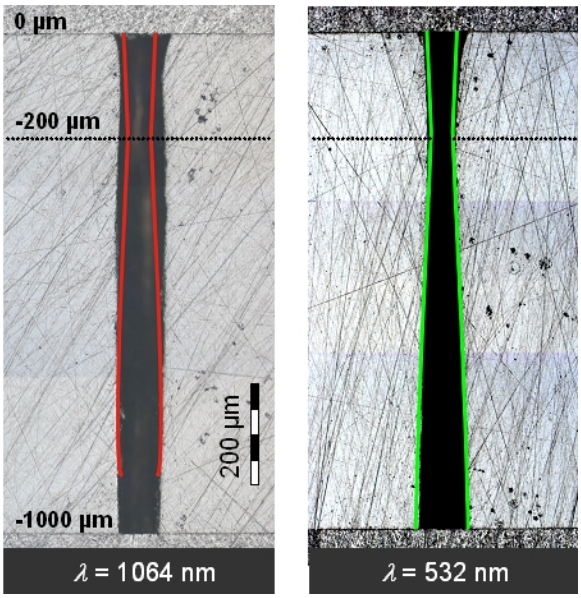

Fig. 8 Comparison of 5 J/cm^2 isophote and hole morphology at 1064 nm (left) and 532 nm (right). 1ω and 2ω: f_p = 40 kHz, Q_p = 80 µJ, f = 100 mm, s = 1 mm, z_f = -200 µm. 1ω: t_D = 120 s, d_f = 19.8 µm. 2ω: t_D = 60 s, d_f = 15.4 µm. The focal position is marked with a dotted line.

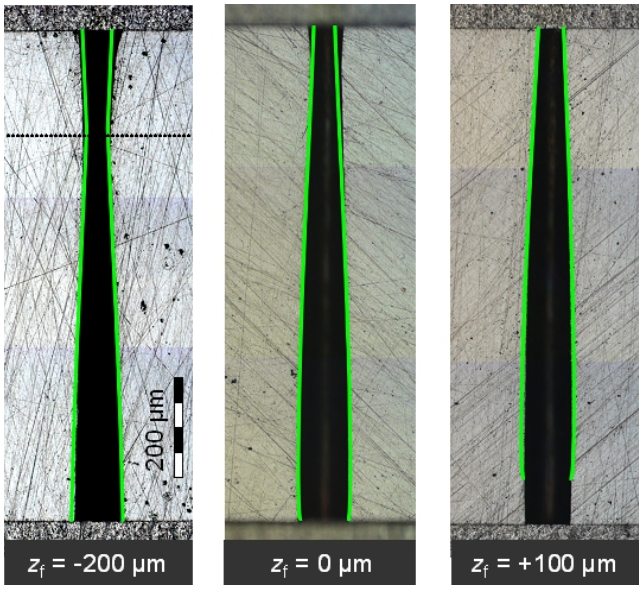

Fig. 9 Comparison of 5 J/cm^2 isophote and hole morphology for different focal positions. λ = 532 nm, f_p = 40 kHz, f = 100 mm, s = 1 mm, t_D = 60 s, d_f = 15.4 µm, H = 43 J/cm^2.

breakdown of air inside the capillary. The energy density (26 J/cm^2 at 1064 nm and 43 J/cm^2 at 532 nm) exceeds the relevant breakdown threshold at both wavelengths. At 532 nm however, a smaller fraction of the pulse energy is transferred to the plasma, causing less radial expansion. Moreover, the reduced plasma absorption at 532 nm leads to less post heating of the bulk material, which finally results in reduced melt generation (compare Sec. 4.2). These findings can be seen as a confirmation of the aforementioned assumption that inverse bremsstrahlung absorption dominates the laser-plasma interaction in the investigated parameter regime.

As described in [5], the plasma cloud builds up in the zone of highest energy density. Fig. 8 confirms that the etching zone corresponds to the position of the beam waist (z_R = 220 µm for the IR beam). The energy that is transferred to the particle-ignited plasma in the upper zone of the capillary is not available for widening the outlet zone [6]. This is a further reason for the smaller outlet diameter and the lower process efficiency achieved with 1064 nm radiation.

Fig. 9 shows transverse sections of microholes which have been fabricated with frequency-doubled radiation at different focal positions. The congruency of isophote contour and hole shape increases with rising focal position. At z_f = +100 µm the hole shape is exclusively determined by the laser beam. This could enable predicting or even designing the hole shape by calculating the isophotes on the basis of the parameters of the laser beam, the focusing optic and the HDO.

Plasma shielding at fundamental wavelength may also contribute to the difference in drilling rates as shown in Figs. 4 and 5. As also stated in [5] however, it is not to be regarded as the principal reason for the drop in drilling rate as it generally occurs at deep hole drilling, because the drop is observed for drilling with both fundamental and frequency-doubled radiation.

5. Conclusion

This paper reveals that, at microdrilling with picosecond laser pulses, a substantial enhancement of precision and efficiency can be achieved by drilling with frequency-doubled radiation. Microholes with a diameter of 100 µm in 1 mm steel can be completed several times faster at 532 nm than at 1064 nm. At 1064 nm, we observe melt ridges and insufficient widening of the outlet, accompanied by poor roundness. The microholes fabricated using the second harmonic though, show a regular shape, smooth hole walls and an absence of recast. Moreover, at 532 nm the drilling process has higher reproducibility due to steadier progression.

We have found that the influence of particle-ignited atmospheric plasma can be minimized by reducing the processing wavelength. At 1064 nm, a considerable part of the laser energy is absorbed by the plasma causing a radial expansion of the upper zone of the capillary, insufficient widening of the outlet as well as the formation of melt due to prolonged surface heating. At 532 nm however, plasma expansion and melt production are negligible. The hole morphology follows the 5 J/cm^2 isophote contour, whereas at 1064 nm ablation takes place beyond the corresponding isophote.

Acknowledgments

The authors wish to thank the German Ministry for Education and Research (BMBF) for funding the project PROMPTUS (13N8583). The authors are responsible for the content.

References

[1] Föhl, C.; Breitling, D.; Dausinger, F.: Precise drilling of steel with ultrashort pulsed solid-state lasers. In: Laser Processing of Advanced Materials and Laser Microtechnologies (LAT 2002). Bellingham (WA): SPIE, 2003, pp. 271-279 (Proc. of SPIE Vol. 5121).

[2] Dausinger, F.; Lichtner, F.; Lubatschowski, H. (Edtrs.): Femtosecond Technology for Technical and Medical Applications. Top. Appl. Phys. **96**, 2004, pp. 131-154.

[3] Dausinger, F.; Schmitz, G.; Sutter, D.: Femtonische Laser im Maschinenbau – Mikrostrukturieren und Bohren. Laser Technik Journal **4**, 2005, pp. 40-47.

[4] Dausinger, F.; Hügel, H.; Konov, V: Micromachining with ultrashort laser pulses: From basic understanding to technical applications. In: Intl. Conference on Advanced Laser Technologies (ALT´02). Bellingham (WA): SPIE, 2003, pp. 106-115 (Proc. of SPIE Vol. 5147).

[5] Kononenko, T.; Klimentov, S.; Konov, V.; Pivovarov, P.; Garnov, S.; Dausinger, F.; Breitling, D.: Propagation of short-pulsed laser radiation and stages of ablative deep-channel formation. In: Laser Applications in Microelectronic and Optoelectronic Manufacturing VI. Bellingham (WA): SPIE, 2001, pp. 248-257 (Proc. of SPIE Vol. 4274).

[6] Klimentov, S.; Kononenko, T.; Pivovarov, P.; Garnov, S.; Konov, V.; Prokhorov, A.; Breitling, D.; Dausinger, F.: The role of plasma in ablation of materials by ultrashort laser pulses. In: Proc. First Intl. WLT-Conference on Lasers in Manufacturing 2001 (München, Germany). Stuttgart, Germany: AT-Fachverlag, 2001, pp. 273-283.

[7] Walter, D.; Kononenko, T.; Michalowski, A.: To be published.

[8] Kononenko, T.; Konov, V.; Garnov, S.; Danielius, R.; Piskarskas, A.; Tamoshauskas, G.; Dausinger, F.: Comparative study of the ablation of materials by femtosecond and pico- or nanosecond laser pulses. Quantum Electronics **29** (8), 1999, pp. 724-728.

[9] Chang, J.; Warner, B.; Dragon, E.; Martinez, M.: Precision micromachining with pulsed green lasers. J. Laser Applications **10** (6), 1998, pp. 285-291.

[10] Le Drogoff, B.; Margot, J.; Vidal, F.; Laville, S.; Chaker, M.; Sabsabi, M.; Johnston, T.; Barthélemy, O.: Influence of the laser pulse duration on laser-produced plasma properties. Plasma Sources Sci. Technol. **13**, 2004, pp. 223-230.

[11] Hügel, H.; Dausinger, F.: Fundamentals of laser-induced processes. In: Martienssen, W. (Edtr.): Laser Physics and Applications. Berlin: Springer, 2004, pp. 3-71 (Landolt-Börnstein: Numerical Data and Functional Relationships in Science and Technology – New Series VIII/1C).

[12] Breitling, D.; Ruf, A.; Dausinger, F.: Fundamental aspects in machining of metals with short and ultrashort laser pulses. In: Photon Processing in Microelectronics and Photonics III. Bellingham (WA): SPIE, 2004, pp. 49-63 (Proc. of SPIE Vol. 5339).

[13] Kleinbauer, J.; Knappe, R.; Wallenstein, R.: A powerful diode-pumped laser source for micro-machining with ps pulses in the infrared, the visible and the ultraviolet. Appl. Phys. B **80**, 2005, pp. 315-320.

[14] Liu, J.M.: Simple technique for measurements of Gaussian-beam spot sizes. Opt. Lett. **7** (5), 1982, pp. 196-198.

[15] Sommer, S.; Kraus, M.; Dausinger, F.: Surface structuring of technical metal surfaces with ultrashort laser pulses – enhancement of quality and efficiency. In: Proc. Fourth Intl. WLT-Conference on Lasers in Manufacturing 2007 (München, Germany). Stuttgart, Germany: AT-Fachverlag, 2007, pp. 557-562.

[16] Kraus, M.; Collmer, S.; Sommer, S.; Michalowski, A.; Dausinger, F.: Microdrilling in steel with ultrashort laser pulses at 1064 nm and 532 nm. In: Proc. Fourth Intl. WLT-Conference on Lasers in Manufacturing 2007 (München, Germany). Stuttgart, Germany: AT-Fachverlag, 2007, pp. 639-644.

(Received: May 23, 2007, Accepted: April 30, 2008)